

Express Letter

Ab initio elasticity and thermal equation of state of MgSiO₃ perovskite

Artem R. Oganov*, John P. Brodholt, G. David Price

Department of Geological Sciences, University College London, Gower Street, London WC1E 6BT, UK

Received 25 September 2000; received in revised form 23 November 2000; accepted 26 November 2000

Abstract

We have used high-temperature ab initio molecular dynamic simulations to study the equation of state of orthorhombic MgSiO₃ perovskite under lower mantle pressure–temperature conditions. We have determined the Grüneisen parameter, γ , as a function of volume. Our state-of-the-art simulations, accurate to within 10%, resolve the long-standing controversy on thermal expansion (α) and Grüneisen parameter of MgSiO₃ perovskite. Under ambient conditions we find the values for α and γ of $1.86 \times 10^{-5} \text{ K}^{-1}$ and 1.51, respectively, in excellent agreement with the latest experimental studies. Calculated elastic constants and the static equation of state at 0 K agree well with previous simulations. We have found no evidence for the high-temperature phase transitions of orthorhombic MgSiO₃ perovskite to cubic or tetragonal phases at mantle temperatures. © 2001 Elsevier Science B.V. All rights reserved.

Keywords: perovskite; lower mantle; equations of state; thermal expansion; elastic constants; Grüneisen parameters; thermoelastic properties

1. Introduction

Despite the fact that (Mg,Fe)SiO₃ perovskite (Mg-pv) is the major phase in the lower mantle, many of its physical properties are still relatively poorly known. For example, its equation of state (EOS) is relatively well known only at 298 K [1,2], while at lower mantle pressures *and* temperatures different experiments are in strong disagreement with each other. Elastic constants have been studied experimentally only under ambient conditions [3], and the thermal expansion of Mg-pv,

crucial for models of the lower mantle composition and dynamics, is poorly known even under ambient conditions (for a discussion see [4]). For the Grüneisen parameter, γ , the reported values under ambient conditions are scattered between 1.2 and 2.0, and its volume dependence parameter, $q = d \ln \gamma / d \ln V$, is uncertain, roughly between 1 and 2.5.

Here we report on our ab initio calculations of the static EOS and elastic properties, and ab initio molecular dynamic (AIMD) simulations of thermal expansion and the Grüneisen parameter, $\gamma(V)$. Compared to previous calculations [5–9] we take advantage of recent advances in quantum mechanics: derivation of the gradient corrected density functionals [10], ultrasoft pseudopotentials [11], and their implementation in the fast and sta-

* Corresponding author. Tel.: +44-20-7679-3344;
Fax: +44-20-7387-1612; E-mail: a.oganov@ucl.ac.uk

ble VASP code [12]. These advances allowed us to perform accurate and efficient calculations of the EOS of Mg-pv, its elastic constants and the first realistic AIMD simulations of this phase under lower mantle P/T conditions.

2. Computational methodology

Our plane wave pseudopotential calculations were performed on the CRAY T3E supercomputer at Manchester Computer Centre. The pseudopotentials for Mg and Si are norm-conserving [13] with partial core corrections, while an ultrasoft pseudopotential was used for O. All the pseudopotentials are non-local. The core radii are 1.06 Å for Mg (valence configuration $3s^23p^03d^0$), 0.95 Å for Si ($3s^23p^23d^0$) and 0.82 Å for O ($2s^22p^43d^0$). The use of an ultrasoft pseudopotential for oxygen allowed us to use a relatively small basis set with the plane wave cut-off energy of 500 eV without any loss of accuracy and with excellent convergence of all properties with respect to the basis set size (the Pulay stress was only 0.05 GPa).

2.1. Static elastic constants and static EOS

A $2 \times 2 \times 2$ mesh for the Brillouin zone sampling and full symmetry were used. The ground state was found by solving the Kohn–Sham equations self-consistently to within 5×10^{-10} eV/atom; the structure was optimised using conjugate gradients to within 5×10^{-10} eV/atom. Elastic constants (C_{ij}) were calculated from non-linear stress–strain relations [9]. These calculations were performed at nine pressures in the pressure range of -17 to 150 GPa. The bulk and shear moduli K and G , obtained as Voigt–Reuss–Hill averages, were used for calculating compressional (V_P) and shear (V_S) sound velocities.

2.2. AIMD simulations

We used an 80-atom supercell ($2a \times 2b \times 1c$ $Pbnm$ -supercell), Γ -point for the Brillouin zone sampling, and a timestep of 1 fs; for each configuration the ground state was found self-consistently to within 6.25×10^{-8} eV/atom. Simulations

were run in the constant NVT ensemble with the Nosé thermostat for at least 0.8 ps after equilibration. The thermostat mass was optimised so as to produce temperature oscillations with a period of atomic vibrations. Our AIMD runs, although relatively short, proved to be sufficient for obtaining well-converged statistical averages for the stress tensor.

2.3. Convergence tests

All computational conditions (plane wave cut-off, Brillouin zone sampling, supercell size, AIMD run length and timestep, thermostat mass, etc.) were carefully tested. Uncertainties in the calculated values are within 1% for diagonal and 2.5% for off-diagonal elastic constants, within 1% for the bulk and shear moduli, and 10% for the Grüneisen parameter.

Table 1
Structure and elasticity of MgSiO_3 perovskite at $P=0$: theory and experiment

Property	LDA ^a	GGA ^b	GGA ^c	Exp. [3,15]
V_0 (Å ³)	162.47	168.04	162.40	162.45
a_0 (Å)	4.7891	4.8337	4.7765	4.7747
b_0	4.9219	4.9830	4.9333	4.9319
c_0	6.8925	6.9767	6.8919	6.8987
C_{11} (GPa)	487	444	493	482
C_{22}	524	489	546	537
C_{33}	456	408	470	485
C_{12}	128	110	142	144
C_{13}	144	126	146	147
C_{23}	156	136	160	146
C_{44}	203	194	212	204
C_{55}	186	172	186	186
C_{66}	145	131	149	147
K (GPa)	257.8	231.3	266.7	264.0
G	174.7	162.3	178.7	177.4
V_P (km/s)	10.935	10.640	11.091	11.042
V_S (km/s)	6.524	6.405	6.598	6.574

^aResults of Karki ([9] and personal communication, 1997).

^bUncorrected GGA (this work).

^cCorrected GGA (this work).

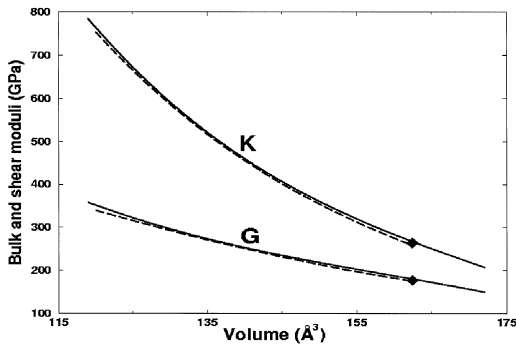


Fig. 1. Bulk and shear moduli of MgSiO₃ perovskite as a function of volume. Solid lines: GGA (this study); dashed lines: LDA (B. Karki, 1997, personal communication), diamonds: experimental data [3].

3. Results and discussion

3.1. Pressure correction

Present-day density functional calculations are known to systematically over- or underestimate the molar volume of solids by a few percent, depending on whether LDA or GGA is used for exchange correlation. This systematic error affects the calculated zero pressure elastic and vibrational properties; more accurate results are obtained when the experimental volume is fixed [14]. Although the pseudopotential LDA calculations of Karki ([9] and personal communication, 1997) give the unit cell volume and elastic constants almost within the experimental uncertainty (Table 1), this is probably because of a cancellation of the LDA- and pseudopotential errors; normally LDA underestimates lattice parameters. As expected, our GGA calculations give unit cell parameters ca. 1% higher and elastic constants some 10–20% lower than the experiment. However, at the experimental unit cell volume (162.4 Å³)¹, GGA yields extremely accurate elastic constants (Table 1) and volume dependences of elastic properties very similar to the LDA results (Fig. 1). Since the GGA calculations correctly reproduce properties at each volume, we can obtain

¹ With the unit cell shape and atomic positions allowed to relax.

the correct pressure dependence of the properties if the GGA pressure is modified to match the true $P(V)$ dependence:

$$P_{\text{total}}^{\text{true}}(V, T) = P_{\text{st}}^{\text{GGA}}(V) + P_{\text{th}}(V, T) - \Delta P(V) \quad (1)$$

A simple constant shift in pressure (ΔP) brings the EOS to excellent agreement with the LDA calculations and experiment (Fig. 2). Matching the ambient conditions volume to 162.4 Å³ and using γ from AIMD (see below) we estimate $\Delta P = 12.08$ GPa; the corrected pressures are used throughout in this paper.

3.2. $\gamma(V)$ from AIMD

The Grüneisen parameter, $\gamma(V)$, was calculated from the thermal pressure: $P_{\text{th}}(V, T) = \gamma(V)E_{\text{th}}(V, T)/V$, where the thermal energy E_{th} is simply $(3N-3)k_{\text{B}}T$ (per supercell containing N atoms) in classical molecular dynamics. Classical approximation always gives the high-temperature limit values for $\gamma(V)$ [17], which is a good approximation even at low temperatures, because γ varies only slightly with T .

The thermal pressure was calculated from the differences in stress tensors obtained in static ($T=0$ K) and AIMD simulations at 500 and 1500 K using lattice parameters optimised at 0 K. Static structure optimisation was performed

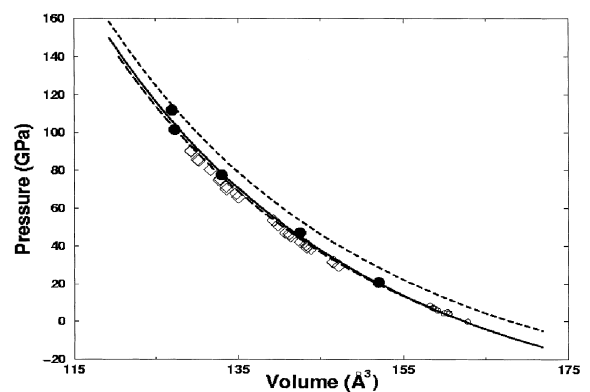


Fig. 2. EOS of MgSiO₃ perovskite. Lower dashed line: athermal LDA (B. Karki, 1997, personal communication), upper dashed line: athermal GGA, solid line: GGA shifted in pressure, effectively at 298 K. Experiments at 298 K: small circles [16], large solid circles [1], diamonds [2].

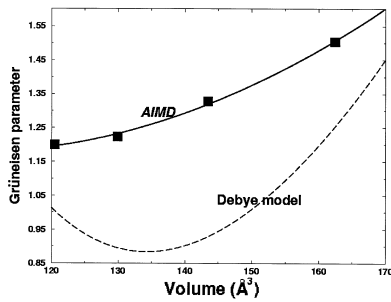


Fig. 3. $\gamma(V)$ function. Solid squares: AIMD results; solid line: best fit ($\gamma = \gamma_0(V/V_0)^{1.27262+1.67772x}$, where $x = \ln(V/V_0)$, $\gamma_0 = 1.506$, $V_0 = 162.40 \text{ \AA}^3$). Dashed curve: Debye model based on ab initio elastic constants.

under the ambient conditions volume and at static pressures of 50, 100 and 150 GPa using the same supercell and computational conditions as in AIMD simulations. Under ambient conditions we find $\gamma_0 = 1.51 \pm 0.1$ similar to 1.5 ± 0.2 preferred in [4]; q varies with volume from 1.27 at 162.4 \AA^3 to 0.26 at 120 \AA^3 . The $\gamma(V)$ calculated from AIMD is shown in Fig. 3; in line with [17], the Debye model gives poor results for $\gamma(V)$.

3.3. Elastic constants and EOS

Table 2 gives elastic constants at pressures up

Table 2
Elastic properties of MgSiO_3 perovskite as a function of pressure (at 298 K)^a

	Pressure (GPa)					
	0	30	60	90	120	150
$V_0 \text{ (\AA}^3\text{)}$	162.4	148.0	138.1	130.6	124.5	119.5
C_{11} (GPa)	492	629	746	851	947	1036
C_{22}	550	727	888	1044	1196	1344
C_{33}	472	661	833	995	1150	1298
C_{12}	142	246	349	449	546	639
C_{13}	148	216	287	360	433	505
C_{23}	160	237	311	385	457	528
C_{44}	213	264	309	351	394	433
C_{55}	187	221	247	272	296	319
C_{66}	154	206	249	293	338	384
K (GPa)	267	379	483	583	681	775
G	180	225	261	294	325	355

^a C_{ij} values in this table were obtained using third order polynomials fitted to the C_{ij} directly calculated at nine pressures between -17 and 150 GPa; elastic constants at 0 GPa differ slightly from those in Table 1.

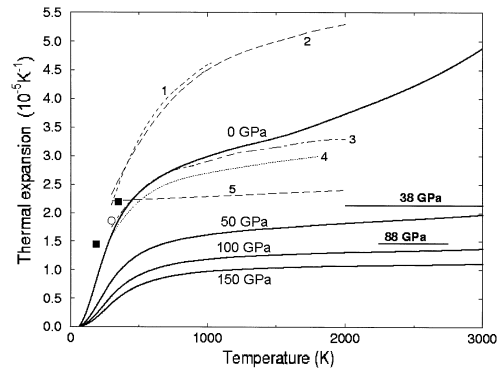


Fig. 4. Thermal expansion of MgSiO_3 perovskite. Solid lines: calculations at 0, 50, 100 and 150 GPa (from the top to the bottom). Empty circle: calculation using γ from AIMD and experimental C_V . Solid horizontal lines: direct AIMD results at 38 and 88 GPa between 1500 and 3500 K. Experimental data at 0 GPa: squares [15], lines 1 [22], 2 [23], 3 [20], 4 [21], 5 [2].

to 150 GPa at 298 K. These are in excellent agreement with previous static LDA calculations [7,9].

Fitting the Vinet EOS [18] to our athermal $P(V)$ data up to 150 GPa, we obtain $V_0 = 160.3 \text{ \AA}^3$, $K_0 = 279.7 \text{ GPa}$ and $K' = 4.02$. On the basis of this static EOS and our calculated $\gamma(V)$ we construct the Mie–Grüneisen thermal EOS:

$$P(V, T) = P_{\text{st}}(V) + \gamma(V)E_{\text{th}}(V, T)/V \quad (2)$$

Table 3
Ab initio thermal EOS of MgSiO₃ perovskite

	<i>T</i> (K)						
	static	0	1500	2000	2500	3000	4000
<i>V</i> ₀ (Å ³)	160.2	162.1	167.9	170.9	174.2	177.9	187.2
<i>K</i> ₀ (GPa)	279.7	269.9	228.3	210.6	192.3	173.5	134.4
<i>K</i> '	4.02	4.07	4.36	4.49	4.63	4.78	5.13

Unlike $\gamma(V)$, thermal EOS cannot be calculated within the classical approximation; one needs to go beyond classical molecular dynamics and introduce quantum corrections in E_{th} . We did this using the Debye model for E_{th} : although crude for γ , it gives accurate heat capacity, C_V , and E_{th} for Mg-pv above 500 K [17] and correct low-temperature behaviour. Errors in the EOS due to the use of the Debye model are within 0.2 GPa and tend to zero at high temperatures. At room temperature $V_0 = 162.4 \text{ \AA}^3$ (fixed), $K_0 = 266.7 \text{ GPa}$, $K' = 4.10$. EOS parameters at several other temperatures are listed in Table 3.

3.4. Thermal expansion

Calculating thermal expansion as $\alpha = \gamma C_V / K_T V$, under ambient conditions we obtain $\alpha_0 = 1.60 \times 10^{-5} \text{ K}^{-1}$ if the heat capacity C_V was obtained using the Debye model, or $1.86 \times 10^{-5} \text{ K}^{-1}$ with experimental C_V [19]. In Fig. 4 we com-

pare our calculated thermal expansion with several experimental sets. Our results strongly support the lower experimental values [2,20,21]. Table 4 gives a summary of thermoelastic parameters of Mg-pv in comparison to several ab initio and experimental studies.

Using AIMD, we optimised the cell parameters at five points, (1500 K; 38 GPa), (2500 K, 38 GPa), (3500 K; 38 GPa), (1500 K; 88 GPa) and (3500 K; 88 GPa), by making the stress tensor equivalent to the target pressure to within 1 GPa. Thermal expansion values, determined directly from the optimised cell volumes, are consistent with those determined from γ to within several percent. The equilibrium cell remained orthorhombic even at the highest probed temperatures, suggesting that phase transitions to a cubic or tetragonal phase are unlikely within the lower mantle. However, other factors (system size, kinetics, defects) still need to be analysed to make the final conclusion.

Table 4
Thermoelastic parameters of MgSiO₃ perovskite from theory and experiment

Source	<i>V</i> ₀ (Å ³)	<i>K</i> ₀ (GPa)	<i>K</i> ' (10 ⁻³ GPa/K)	($\partial K_T / \partial T$) _P (10 ⁻⁵ K ⁻¹)	$\partial^2 K_T / \partial P \partial T$	γ_0	<i>q</i>	α_0 (10 ⁻⁵ K ⁻¹)
<i>Ab initio simulations:</i>								
LDA [8]	160.74	266	4.2	–	–	–	–	–
LDA [6]	157.50	259	3.9	–	–	–	–	–
LDA ^a	162.47	257	4.02	–	–	–	–	–
GGA (this work)	(162.4)	267	4.10	–21	15	1.51	1.27 to 0.26	1.86
<i>Experiment:</i>								
[2]	162.3	259.5	3.69	–17	–	(1.4)	1.4	1.8–2.2
[24]	(162.3)	(261)	(4)	–28	–	1.42	2.0	1.7
[25] ^b	(162.2)	(261)	(4)	–22	8	1.25	1	1.65
Experimental range	162.4 ± 1	247–272	3.6–7	–17 to –63	–	1.3–2.2	~ 1–2.5	1.4–3.3

^aResults of Karki ([9] and personal communication, 1997).

^bApproach in [25], based on Raman spectroscopic measurements combined with experimental room temperature EOS, resulted in several distinct models. Numbers given here correspond to the model preferred in [25].

Acknowledgements

A.R.O. would like to acknowledge funding from the Russian President Scholarship for Education Abroad, UCL Graduate School Research Scholarship, and UK Overseas Research Scholarship. J.P.B. gratefully acknowledges the receipt of a Royal Society University Research fellowship. We thank Georg Kresse for the use of the VASP code, Mike Gillan for discussions, and anonymous reviewers for constructive suggestions on the manuscript. Access to the supercomputing facilities was provided by the NERC. [AH]

References

- [1] E. Knittle, R. Jeanloz, Synthesis and equation of state of (Mg,Fe)SiO₃ perovskite to over 100 GPa, *Science* 235 (1987) 668–670.
- [2] G. Fiquet, A. Dewaele, D. Andrault, M. Kunz, T. Le Bihan, Thermoelastic properties and crystal structure of MgSiO₃ perovskite at lower mantle pressure and temperature conditions, *Geophys. Res. Lett.* 27 (2000) 21–24.
- [3] A. Yeganeh-Haeri, Synthesis and re-investigation of the elastic properties of single-crystal magnesium silicate perovskite, *Phys. Earth Planet. Int.* 87 (1994) 111–121.
- [4] O.L. Anderson, K. Masuda, D.W. Guo, Pure silicate perovskite and the PREM lower mantle model: a thermodynamic analysis, *Phys. Earth Planet. Int.* 89 (1995) 35–49.
- [5] R.M. Wentzcovitch, J.L. Martins, G.D. Price, Ab initio molecular dynamics with variable cell shape: application to MgSiO₃, *Phys. Rev. Lett.* 70 (1993) 3947–3950.
- [6] R.M. Wentzcovitch, N.L. Ross, G.D. Price, Ab initio study of MgSiO₃ and CaSiO₃ perovskites at lower-mantle pressures, *Phys. Earth Planet. Int.* 90 (1995) 101–112.
- [7] R.M. Wentzcovitch, B.B. Karki, S. Karato, C.R.S. da Silva, High pressure elastic anisotropy of MgSiO₃ perovskite and geophysical implications, *Earth Planet. Sci. Lett.* 164 (1998) 371–378.
- [8] L. Stixrude, R.E. Cohen, Stability of orthorhombic MgSiO₃ perovskite in the Earth's lower mantle, *Nature* 364 (1993) 613–616.
- [9] B.B. Karki, L. Stixrude, S.J. Clark, M.C. Warren, G.J. Ackland, J. Crain, Elastic properties of orthorhombic MgSiO₃ perovskite at lower mantle pressures, *Am. Miner.* 82 (1997) 635–638.
- [10] Y. Wang, J.P. Perdew, Correlation hole of the spin-polarized electron gas, with exact small-vector and high-density scaling, *Phys. Rev. B* 44 (1991) 13298–13307.
- [11] D. Vanderbilt, Soft self-consistent pseudopotentials in a generalized eigenvalue problem, *Phys. Rev. B* 41 (1990) 7892–7895.
- [12] G. Kresse, J. Furthmüller, Efficiency of ab initio total-energy calculations for metals and semiconductors using a plane-wave basis set, *Comp. Mater. Sci.* 6 (1996) 15–50.
- [13] A.M. Rappe, K.M. Rabe, E. Kaxiras, J.D. Joannopoulos, Optimized pseudopotentials, *Phys. Rev. B* 41 (1990) 1227–1230.
- [14] D. Vanderbilt, First-principles theory of structural phase transitions in cubic perovskites, *J. Korean Phys. Soc.* 32 (1998) S103–S106.
- [15] N.L. Ross, R.M. Hazen, Single crystal X-ray diffraction study of MgSiO₃ perovskite from 77 to 400 K, *Phys. Chem. Miner.* 16 (1989) 415–420.
- [16] T. Yagi, H.K. Mao, P.M. Bell, Hydrostatic compression of perovskite-type MgSiO₃, in: S.K. Saxena (Ed.), *Advances in Physical Geochemistry*, Vol. 2, Springer, Berlin, 1982, pp. 317–325.
- [17] A.R. Oganov, J.P. Brodholt, G.D. Price, Comparative study of quasiharmonic lattice dynamics, molecular dynamics and Debye model applied to MgSiO₃ perovskite, *Phys. Earth Planet. Int.* 122 (2000) 277–288.
- [18] P. Vinet, J.H. Rose, J. Ferrante, J.R. Smith, Universal features of the equation of state of solids, *J. Phys. Cond. Matter* 1 (1989) 1941–1963.
- [19] M. Akaogi, E. Ito, Heat capacity of MgSiO₃ perovskite, *Geophys. Res. Lett.* 20 (1993) 105–108.
- [20] Y. Wang, D.J. Weidner, R.C. Liebermann, Y. Zhao, *P–V–T* equation of state of (Mg,Fe)SiO₃ perovskite: constraints on composition of the lower mantle, *Phys. Earth Planet. Int.* 83 (1994) 13–40.
- [21] N. Funamori, T. Yagi, W. Utsumi, T. Kondo, T. Uchida, Thermoelastic properties of MgSiO₃ perovskite determined by in situ X-ray observations up to 30 GPa and 2000 K, *J. Geophys. Res.* 101 (1996) 8257–8269.
- [22] E. Knittle, R. Jeanloz, Thermal expansion of silicate perovskite and stratification of the Earth's mantle, *Nature* 319 (1986) 214–216.
- [23] H.K. Mao, R.J. Hemley, Y. Fei, J.F. Shu, L.C. Chen, A.P. Jephcoat, Y. Wu, Effect of pressure, temperature, and composition on lattice parameters and density of (Mg,Fe)SiO₃-perovskites to 30 GPa, *J. Geophys. Res.* 96 (1991) 8069–8079.
- [24] S.-H. Shim, T.S. Duffy, Constraints on the *P–V–T* equation of state of MgSiO₃ perovskite, *Am. Miner.* 85 (2000) 354–363.
- [25] P. Gillet, I. Daniel, F. Guyot, J. Matas, J.-C. Chervin, A thermodynamic model for MgSiO₃-perovskite derived from pressure, temperature and volume dependence of the Raman mode frequencies, *Phys. Earth Planet. Int.* 117 (2000) 361–384.